

## Reflection of regular and irregular waves from a partially perforated caisson breakwater with a rock-filled core

LIU Yong<sup>1</sup>, LI Yucheng<sup>1, 2\*</sup>, TENG Bin<sup>1</sup>, MA Baolian<sup>3</sup>

1. State Key Laboratory of Coastal and Offshore Engineering, Dalian University of Technology, Dalian 116024, China

2. R&D Center for Civil Engineering Technology, Dalian University, Dalian 116622, China

3. Tianjin Maritime Safety Administration, Tianjin 300456, China

Received 14 May 2006; accepted 10 September 2006

### Abstract

The reflection of regular and irregular waves from a partially perforated caisson breakwater with a rock-filled core is examined. The present mathematical model is developed by means of the matched eigenfunction method. Numerical results of the present model are compared with the experimental data of different researchers. Numerical examples are given to examine the effect of rock fill on the reflection coefficient. The differences between regular and irregular waves are also investigated by means of theoretical and experimental results. It is found that the minimum reflection coefficient of irregular waves is larger than that of corresponding regular waves, but the contrary is the case for the maximum reflection coefficient.

**Key words:** reflection coefficient, regular waves, irregular waves, partially perforated caisson, rock fill

## 1 Introduction

Recently perforated caissons are often used to construct vertical breakwaters and wharfs in coastal engineering as they can effectively reduce the wave reflection and wave forces on the structures. Owing to the stability requirements of the structures, the front wall of the caisson is usually partially perforated above a certain level, and the caisson chamber below the perforated part of the front wall is generally filled with large diameter rocks. For example, in Dalian in China, the wharfs (9 – 16) in the Dayao

Bay Harbor and the breakwater for the COSCO Shipyard have been both constructed with partially perforated caissons. The reduction in wave reflection and wave forces could be obtained and has resulted in a considerable reduction in the total costs of the project.

A perforated wall breakwater consisting of a perforated front wall, a solid back wall and a wave absorbing chamber between them was initially proposed by Jarlan (1961). Since then, the Jarlan-type structure has received considerable attention due to its significant wave absorbing performance. The correlative research projects mainly focused on the interaction of regular waves with fully perforated wall structures (Chwang and Dong, 1984; Twu and

---

\* Corresponding author, E – mail: liyuch@dlut.edu.cn

Lin, 1991; Fugazza and Natale, 1992; Sahoo et al., 2000) as well as partially perforated wall breakwaters (Tanimoto and Yoshimoto, 1982; Chen et al., 2002; Li et al., 2002, Li et al., 2005). Moreover, several researchers have studied the irregular wave reflection from perforated breakwaters. Tanimoto et al. (1976) investigated the reflection of irregular waves from a fully perforated caisson breakwater by means of a series of experimental tests. Bennett et al. (1992) presented an analytical model to predict the reflection of regular and irregular waves from a fully perforated breakwater and carried out experiments to validate their model. Suh et al. (2001) also developed a similar model by using more complicated matching boundary conditions, and validated their model by means of experiments. More recently, Suh et al. (2006) have presented a numerical model to calculate the reflection coefficients of regular and irregular waves from a partially perforated breakwater mounted on a solid mound foundation. In their model, the imperforated part of the front wall was assumed to be a very steep slope.

The aforementioned analytical models with respect to partially perforated breakwaters dealt with the case that in the caisson chamber below the perforated wall, the bottom is solid. Liu et al. (2006) have investigated the regular wave forces on a partially perforated breakwater with a rock-filled core. In the present study, our interests focus on the reflection of both regular and irregular waves by the same structure. Therefore, the mathematical model of Liu et al. (2006), which has been developed based on the eigenfunction expansion method (Isaacson et al., 2000; Sahoo et al., 2000; Song and Sun, 2006; Teng et al., 2006), is further developed to estimate the reflection coefficients of regular and irregular waves.

## 2 Mathematical model

The idealized geometry of the problem is shown in Fig. 1. A normally incident, regular or irregular wave train approaches a partially perforated caisson breakwater with a rock-filled core. The water depth is assumed to be constant and represented with  $h$ . The front wall is partially perforated from a distance ( $b$ ) below the still water level to the top, and the rock fill thickness is  $a$ ; therefore  $h = a + b$ . The width of the wave absorbing chamber is  $B$ . A Cartesian-coordinate system  $Oxz$  is defined with the origin at the intersection of the chamber rear wall and the still water level, the  $z$ -axis directing vertically upwards and the  $x$ -axis directing out of the fluid domain. The whole fluid domain is divided into three sub-regions; Region 1, the fluid domain in front of the perforated caisson; Region 2, the fluid domain above the rock fill in the wave absorbing chamber; Region 3, the fluid domain occupied by the rock fill. The thickness of the perforated front wall is assumed to be 0 as it is very small compared with the incident wavelength.

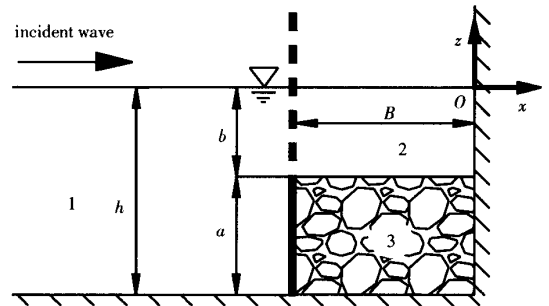


Fig. 1. Definition sketch.

### 2.1 Regular waves

It is assumed that the fluid is inviscid, incompressible, and its motion is irrotational in the whole fluid domain. Then, the velocity potential  $\Phi(x, z, t)$

can be used to describe the wave motions inside and outside the porous medium ( Sollitt and Cross, 1972). For monochromatic incident waves with an angular frequency ( $\omega$ ), the time factor  $e^{-i\omega t}$  can be separated out and so the velocity potential can be written as

$$\Phi(x, z, t) = \text{Re}[\phi(x, z)e^{-i\omega t}], \quad (1)$$

where,  $\text{Re}[\ ]$  denotes the real part of the argument;  $i = \sqrt{-1}$ , is the imaginary unit;  $t$  is the time; and  $\phi$  denotes the spatial velocity potential. In each sub-region, the spatial potential satisfies the Laplace equation

$$\frac{\partial^2 \phi_j(x, z)}{\partial x^2} + \frac{\partial^2 \phi_j(x, z)}{\partial z^2} = 0, \quad j = 1, 2, 3 \quad (2)$$

where the subscript  $j$  represents variables with respect to Region  $j$ .

The spatial potentials are also required to satisfy appropriate boundary conditions on the free surface, water bottom, solid back wall and the interfaces between different regions:

$$\frac{\partial \phi_j}{\partial z} = \frac{\omega^2}{g} \phi_j, \quad z = 0, \quad j = 1, 2, \quad (3)$$

$$\frac{\partial \phi_j}{\partial z} = 0, \quad z = -h, \quad j = 1, 3, \quad (4)$$

$$\frac{\partial \phi_j}{\partial x} = 0, \quad x = 0, \quad j = 2, 3, \quad (5)$$

$$\frac{\partial \phi_2}{\partial z} = \varepsilon_r \frac{\partial \phi_3}{\partial z}, \quad z = -b, \quad (6)$$

$$\phi_2 = (s_r + if_r) \phi_3, \quad z = -b, \quad (7)$$

$$\frac{\partial \phi_1}{\partial x} = \frac{\partial \phi_2}{\partial x} = ik_0 G(\phi_1 - \phi_2), \quad x = -B, \quad -b \leq z \leq 0, \quad (8)$$

$$\frac{\partial \phi_1}{\partial x} = \frac{\partial \phi_3}{\partial x} = 0, \quad x = -B, \quad -h \leq z \leq -b, \quad (9)$$

where  $g$  is the gravitational acceleration; the subscript  $r$  represents variables with respect to the rock fill;  $\varepsilon$ ,  $s$  and  $f$  denote, respectively, the porosity, the inertial effect coefficient and the linearized resistance coefficient of porous medium;  $k_0$  is the inci-

dent wavenumber;  $G$  is the porous effect parameter defined by Chwang (1983) and modified by Yu (1995) as

$$G = \frac{\varepsilon_w}{k_0 \delta (f_w - is_w)} \quad (10)$$

in which, the subscript  $w$  represents variables with respect to the perforated front wall which is also treated as a porous medium; and  $\delta$  is the perforated wall thickness. It should be pointed out that, although the perforated wall thickness is treated as 0 when considering the wave interaction with the breakwater, the thickness of the wall is considered nonzero for the flow within the perforated wall.

It is noted that Eqs (6) and (7) denote the vertical mass flux and dynamic pressure continuous conditions between Regions 2 and 3, respectively. Equation (8) is the porous boundary condition derived by Yu (1995). The first part of Eq. (8) indicates that the horizontal mass fluxes between the Regions 1 and 2 must be continuous at the perforated front wall. The second part indicates that the normal fluid velocity passing through a thin perforated wall is linearly proportional to the pressure difference between the two sides of the wall under the linear assumption.

By the separation of variables, the velocity potentials satisfying the Laplace equation and the relevant boundary conditions, Eqs (3) ~ (7), can be written as

$$\phi_1 = -\frac{igH}{2\omega} \left[ e^{ik_0(x+B)} \frac{\cosh k_0(z+h)}{\cosh k_0 h} + R_0 e^{-ik_0(x+B)} \frac{\cosh(z+h)}{\cosh k_0 h} + \sum_{m=1}^{\infty} R_m e^{k_m(x+B)} \frac{\cos k_m(z+h)}{\cos k_m h} \right], \quad (11)$$

$$\phi_2 = -\frac{igH}{2\omega} \sum_{n=0}^{\infty} A_n \cos(\lambda_n x) \times \frac{\cosh \lambda_n(z+h) - P_n \sinh \lambda_n(z+h)}{\cosh \lambda_n h - P_n \sinh \lambda_n h}, \quad (12)$$

$$\phi_3 = -\frac{igH}{2\omega} \sum_{n=0}^{\infty} A_n \cos(\lambda_n x) \frac{1 - P_n \tanh \lambda_n a}{s_r + if_r} \times$$

$$\frac{\cosh\lambda_n(z+h)}{\cosh\lambda_n h - P_n \sinh\lambda_n h}, \tag{13}$$

where  $H$  is the incident wave height; and

$$P_n = \frac{(1 - \frac{\varepsilon_r}{s_r + if_r}) \tanh\lambda_n a}{1 - \frac{\varepsilon_r}{s_r + if_r} \tanh^2\lambda_n a}. \tag{14}$$

The wavenumbers  $k_0$  and  $k_m$  are the positive real roots of the following dispersion relations

$$\omega^2 = gk_0 \tanh k_0 h = -gk_m \tanh k_m h, \tag{15}$$

$$m = 1, 2, \dots$$

The complex wavenumbers  $\lambda_n$  satisfy the following complex dispersion relations

$$\omega^2 - g\lambda_n \tanh\lambda_n h = P_n (\omega^2 \tanh\lambda_n h - g\lambda_n), \tag{16}$$

$$n = 0, 1, 2, \dots$$

The unknown complex coefficients  $R_m$  and  $A_n$  must be determined by means of the matching boundary conditions, Eqs (8) and (9), at the front wall of the breakwater. The matching method has been explained in detail in another paper (Liu et al., 2006), and is omitted here.

For the regular waves, the real reflection coefficient is defined as the ratio of the reflected wave height to the incident wave height. It is noted that the first part on the right hand side of Eq. (11) represents the incident waves propagating in the positive  $x$ -direction, the second part the reflected waves from the breakwater and the third part a series of evanescent modes decaying in the negative  $x$ -direction. Therefore, the reflection coefficient  $K_r$  of regular waves can be calculated by

$$K_r = |R_0|. \tag{17}$$

To apply the present theoretical solutions to practice, the resistance coefficient  $f$  and the inertial coefficient  $s$  of the porous media need to be determined ahead. In general, the inertial coefficient can be taken to be unity for the rock fill and the perforated wall (Isaacson et al., 2000). For the resistance coefficient  $f_w$  of the perforated front wall, an empirical formula is given by Li et al. (2006) as

$$f_w = -3\,338.7(\delta/h)^2 + 82.769(\delta/h) + 8.711, \tag{18}$$

$$0.0094 \leq \delta/h \leq 0.05.$$

With regard to the resistance coefficient  $f_r$  of the rock fill, an iterative calculation is required through the following formula (Sollitt and Cross, 1972)

$$f_r = \frac{1}{\omega} \frac{\int_V dV \int_t^{t+T} \varepsilon_r^2 (\frac{\nu}{K_p} |q|^2 + \frac{C_t \varepsilon_r}{K_p} |q|^3) dt}{\int_V dV \int_t^{t+T} \varepsilon_r |q|^2 dt}, \tag{19}$$

where  $V$  is the volume of porous medium;  $T$  is the incident wave period;  $\nu$  is the kinetic viscosity of fluid;  $q$  is the real part of the seepage velocity;  $K_p$  is the intrinsic permeability of the material; and  $C_t$  is the turbulent friction coefficient. The intrinsic permeability of the material and the turbulent friction coefficient must be obtained from experiments (Sollitt and Cross, 1972; van Gent, 1995; Requejo et al., 2002).

### 2.2 Irregular waves

An irregular wave train can be treated as a stationary stochastic process. It is assumed to be a linear superposition of large numbers of monochromatic wave components with different wave heights, wave angular frequencies and random initial phases. Thus the total velocity potential  $\Phi'(x, z, t)$  of irregular waves can be written as

$$\Phi'(x, z, t) = \text{Re} [ \sum_{j=1}^J \phi_j(x, z) e^{-i(\omega_j t + \alpha_j)} ], \tag{20}$$

where  $J$  is the total number of wave components which should be infinite theoretically;  $\phi_j$ ,  $\omega_j$  and  $\alpha_j$  are the spatial velocity potential, the angular frequency and the initial phase of the  $j$ th component wave, respectively. The velocity potential  $\phi_j$  of each component of waves also satisfies the Laplace equation and the corresponding boundary conditions described in Section 2.1. So, by neglecting the interaction of different components of waves, the reflection coefficient of each component can be calculated

by means of the above regular wave model. It is noted that in the calculations, the coefficients  $f_r$ ,  $s_r$  and  $G$  should be calculated separately for each wave component. Once the reflection coefficient of each component is determined, the reflected spectral density can be obtained by

$$S_r(\omega_j) = K_j^2 S_i(\omega_j), \quad (21)$$

where  $K_j$  is the reflection coefficient of the  $j$ th component;  $S_r(\omega_j)$  and  $S_i(\omega_j)$  are the spectral densities of the reflected and incident waves, respectively. Here  $K_j$  can be considered as a linear transfer function between the incident and reflected wave spectra.

For irregular waves, the average reflection coefficient  $\bar{K}_r$  can be calculated by

$$\bar{K}_r = \sqrt{\frac{m_{0,r}}{m_{0,i}}}, \quad (22)$$

where  $m_{0,r}$  and  $m_{0,i}$  are the zero-order moments of the reflected and incident wave spectra, respectively, and can be calculated by

$$m_{0,r} = \int_0^\infty S_r(\omega) d\omega, \quad m_{0,i} = \int_0^\infty S_i(\omega) d\omega. \quad (23)$$

In the calculations, the angular frequency range of incident wave spectrum is set from the low frequency  $\omega_l$  to the high frequency  $\omega_h$ . Then  $\mu$  percent energy is neglected both in the ranges of  $[0, \omega_l]$  and  $[\omega_h, +\infty]$ .  $\mu = 0.2$ , it is adopted in the present study (Yu, 2000). Moreover, the incident wave spectrum is equally divided into  $M$  bands in the range of  $[\omega_l, \omega_h]$ . Here  $M = 100$ , it is used and it is sufficiently accurate for calculating the reflection coefficient.

### 3 Validations

#### 3.1 Comparisons with limiting cases

The present model has been validated by comparing the numerical results for limiting cases with the results of Sahoo et al. (2000) and Li et al.

(2002). When the rock fill thickness is 0 ( $a = 0$  and  $h = b$ ), the present structure becomes a fully perforated wall structure as investigated by Sahoo et al. (2000). At this time, the reflection coefficient of regular waves can also be calculated by the formula of Sahoo et al. (2000):

$$K_r = \frac{1 - G(1 - i \cot k_0 B)}{1 + G(1 + i \cot k_0 B)}. \quad (24)$$

Figure 2 shows the comparison of reflection coefficients between the present prediction and the result of Sahoo et al. (2000) for the case of  $k_0 h = 1.3$ ,  $b/h = 1.0$ ,  $\delta/h = 0.025$ ,  $\varepsilon_w = 0.3$ ,  $f_w = 8.7$  and  $s_w = 1.0$ , where  $L$  is the incident wavelength. It can be easily seen from Fig. 2 that these two results are the same. When the porosity of rock fill is 0 ( $\varepsilon_r = 0$  and  $f_r = +\infty$ ), the present structure reduces to a partially perforated wall breakwater with a solid core studied by Li et al. (2002). For this case, the reflection coefficient of regular waves can also be calculated by using the analytical model of Li et al. (2002). Figure 3 shows the comparison between the present prediction and the result of Li et al. (2002) for the case of  $k_0 h = 1.3$ ,  $b/h = 0.5$ ,  $\delta/h = 0.025$ ,  $\varepsilon_w = 0.3$ ,  $f_w = 8.7$ ,  $s_w = 1.0$ ,  $f_r = +\infty$  and  $\varepsilon_r = 0$ . It can be seen from Fig. 3 that these two results are also the same.

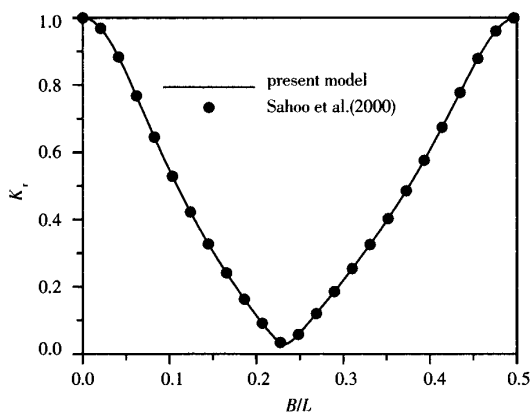


Fig. 2. Comparison between the result of Sahoo et al. (2000) and the present model.

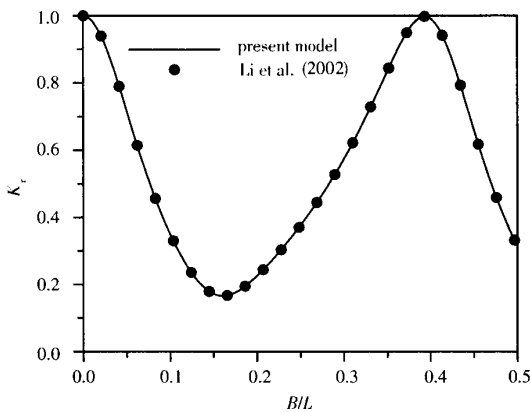


Fig. 3. Comparison between the result of Li et al. (2002) and the present model.

### 3.2 Comparison between experimental and numerical results

Bennett et al. (1992) conducted a series of experimental tests to measure the reflection coefficients of irregular waves from a slotted wave screen with a solid back wall. The tests were designed on a scale of 1 : 15, and two special incident wave spectra named A and B were used in the tests. All the dimensions introduced here refer to the prototype. Spectrum A covered the frequencies equivalent to the wave periods of 4.5 to 14.0 s, and Spectrum B covered 2.9 to 6.2 s. Other experimental conditions were:  $h = b = 8.6$  m,  $B = 5, 10$  and 15 m and  $\varepsilon_w = 0.072, 0.148$  and 0.209. The experimental data of Bennett et al. (1992) were analyzed by them through Fourier analysis, and the spectra of reflection coefficients were provided in their paper.

The thickness of the screen was not described in Bennett et al. (1992). Here we adopt a reasonable value of  $\delta = 15$  cm in our calculations. Then the value of  $f_w = 9.14$  is obtained from Eq. (18). Furthermore, the values of  $G$  are determined from Eq. (10) with  $f_w = 9.14$  and  $s_w = 1.0$ . Once the values of  $G$  are obtained, the reflection coefficient spectra can be calculated by using the present regular wave model. Figure 4 shows the comparison between the

predicted and measured spectra of reflection coefficients. Although there are some differences between the predictions and the measurements, the important features of the experimental results can be adequately reproduced, even for those sharply peaked curves. The average reflection coefficients for both Spectra A and B are also calculated by using Eqs (22) and (23). The comparison between the experimental results and the simulated results of the present model is shown in Fig. 5, and the agreement between them is also satisfactory.

Suh et al. (2001) conducted laboratory experiments to measure the reflection coefficients of irregular waves from fully perforated caisson breakwaters. The incident wave spectrum used in their tests was a B - M spectrum with the following form

$$S_i(f') = 0.205 H_s^2 T_s (T_s f')^{-5} \times \exp[-0.75(T_s f')^{-4}], \quad (25)$$

where  $f'$  is the wave frequency;  $H_s$  and  $T_s$  are the significant wave height and the significant wave period, respectively. Other experimental conditions were:  $h = b = 40$  cm,  $B = 15, 30, 45$  and 60 cm,  $\varepsilon_w = 0.333, H_s = 3, 6$  and 9 cm and  $T_s = 1.0 - 2.0$  s.

In the tests of Suh et al. (2001), the perforated front wall thickness and the water depth were 1 and 40 cm, respectively. Therefore, according to Eq. (18),  $f_w = 8.7$  and  $s_w = 1.0$ , they are used in our calculations. Figure 6 shows the comparison between the numerical and experimental results. It is noted that in our calculations, the incident spectrum is determined by means of the measured values of the significant wave height and the significant wave period provided in Suh et al. (2001). It can be seen from Fig. 6 that the overall agreement between the numerical and experimental results is good for the cases of  $H_s = 6$  and 9 cm ( $H_s/h = 0.150$  and 0.225). But the present model somewhat underestimates the reflection coefficients for the case of  $H_s = 3$  cm ( $H_s/h = 0.075$ ). Maybe, this is due to the overprediction

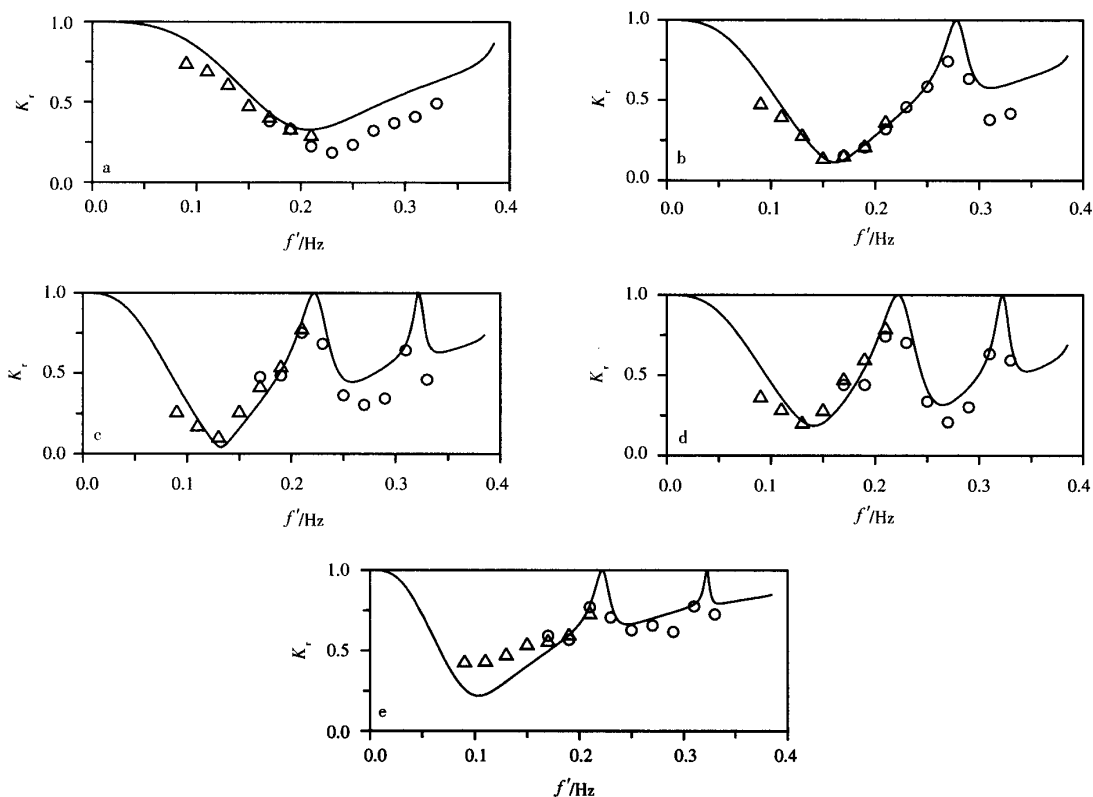


Fig. 4. Comparison of reflection coefficient spectra between present predictions and experimental results of Bennett et al. (1992). a.  $\varepsilon_w = 0.148, B = 5$  m; b.  $\varepsilon_w = 0.148, B = 10$  m; c.  $\varepsilon_w = 0.148, B = 15$  m; d.  $\varepsilon_w = 0.209, B = 15$  m; e.  $\varepsilon_w = 0.072, B = 15$  m. Predictions:  $\circ$  represents Spectrum A and  $\triangle$  Spectrum B. — Experiments.

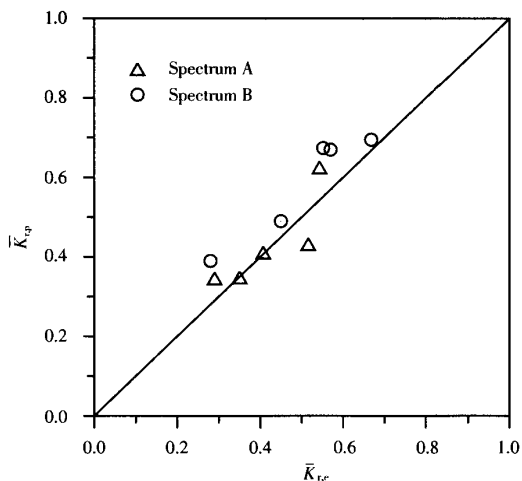


Fig. 5. Comparison of irregular wave reflection coefficients between present predictions ( $\bar{K}_{r,p}$ ) and experimental data ( $\bar{K}_{r,e}$ ) of Bennett et al. (1992).

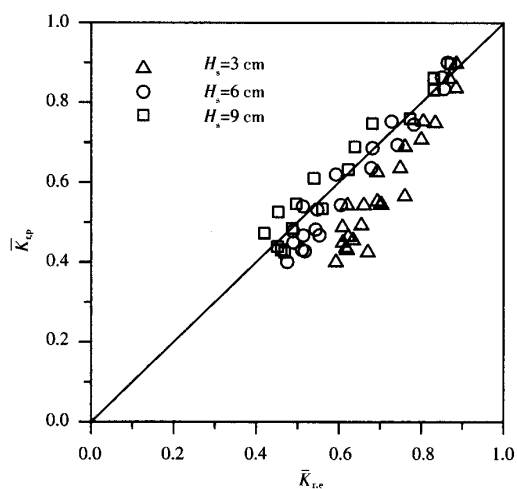


Fig. 6. Comparison of irregular wave reflection coefficients between present predictions and experimental data of Suh et al. (2001).

of the wave energy loss on the perforated front wall when the dimensionless wave height  $H_s/h$  is rather small. In fact, large waves are of more interest for the engineering design, and so the present model should be reliable in practice.

We carried out a series of experimental tests to investigate the interaction of regular and irregular waves with a partially perforated caisson breakwater with a rock – filled core. The experiments were conducted in a wave – current flume in the State Key Laboratory of Coastal and Offshore Engineering, Dalian University of Technology, China. The flume is 56 m long, 0.7 m wide and 1.0 m deep, and equipped with a piston – type irregular wave maker. For the irregular waves, the incident wave spectrum was the modified JONSWAP spectrum (Goda, 1999) given by

$$S_i(f') = \beta_1 H_s^2 T_p^{-4} f'^{-5} \exp[-1.25(T_p f')^{-4}] \times \gamma^{\exp[-(T_p f' - 1)^2/2\sigma^2]}, \quad (26)$$

$$\beta_1 = \frac{0.06238}{0.230 + 0.0336\gamma - 0.185(1.9 + \gamma)^{-1}} \times [1.094 - 0.01915\ln\gamma], \quad (26a)$$

$$T_p = \frac{T_s}{1 - 0.0132(\gamma + 0.2)^{-0.559}}, \quad (26b)$$

$$\sigma = \begin{cases} 0.07 & f' \leq f_p' \\ 0.09 & f' \geq f_p' \end{cases}, \quad (26c)$$

where  $T_p$  and  $f_p'$  denote the wave period and the frequency at the spectral peak, respectively;  $\gamma$  is the peak enhancement factor and its mean value of 3.3 was used in our experiments. Other experimental conditions are listed in Table 1. In the experiments, the reflection coefficients and the wave forces were both measured. The regular wave forces have been analyzed in Liu et al. (2006), and details on the physical model and the experimental set – up can also be found in that paper. Here we use the experimental data of reflection coefficients for regular and irregular waves.

Table 1. Experimental conditions of present model tests

Regular wave $T/s$	0.86	1.0	1.2	1.4
Regular wave $H/cm$	6, 8	6, 8, 10, 12	6, 8, 10, 12	6, 8, 10, 12
Irregular wave $T_s/s$	0.99	1.15		1.38
Irregular wave $H_s/cm$	5.3, 6.7, 8.0	5.3, 6.7, 8.0		5.3, 6.7, 8.0
Water depth $h/cm$	40	perforated wall depth $b$ (cm)		20
Caisson porosity $\epsilon_w$	0.2, 0.4	perforated wall thickness $\delta$ (cm)		1.0
Chamber width $B/cm$		15, 20, 30		

In our tests, the perforated front wall thickness and the water depth were also 1 and 40 cm, respectively. In addition, the porosity and the median grain size of rock fill were 0.447 and 0.9 cm, respectively. This is similar to one of the gravels used by Sollitt and Cross (1972) in their tests. Thus, based on Eq. (18) and Sollit and Cross (1972), the parameters used for the calculations are  $f_w = 8.7$ ,  $s_w = s_r = 1.0$ ,  $K_p = 0.3484 \times 10^{-7} \text{ m}^2$  and  $C_t = 0.406$ . In addition, the value of  $f_r$  is calculated by

Eq. (19) with an iterative procedure. It should be noted that  $f_r$  is relevant to the wave height in theory. But the numerical results show that the effect of wave height on  $f_r$  can be neglected under the present experimental conditions. Therefore, constant dimensionless wave heights  $H/h = 0.2$  and  $H_s/h = 0.17$  are used to calculate  $f_r$  for regular and irregular waves, respectively. The comparison between the experimental and numerical results of  $K_r$  and  $\bar{K}_r$  is shown in Figs 7 and 8, respectively, where  $L_s$  is the

significant wavelength of irregular waves. From Fig. 7, we can see that generally there exists a good agreement between the numerical and experimental results of regular waves. For irregular waves, the numerical results agree with the experimental data very well for  $\varepsilon_w = 0.4$ , as shown in Fig. 8b. But for  $\varepsilon_w = 0.2$ , the present model gives conservative predictions of  $\bar{K}_r$ , compared with the experimental results, as shown in Fig. 8a.

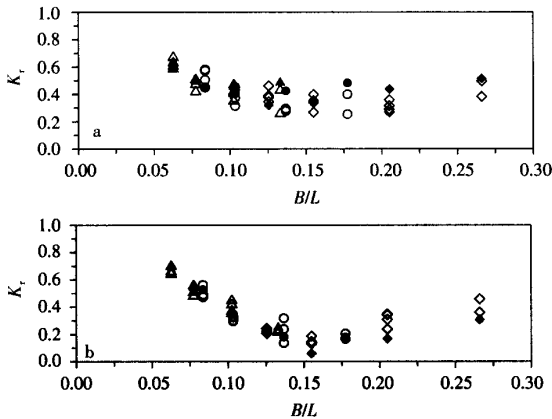


Fig. 7. Comparison of regular wave reflection coefficients between present predictions and experimental results. a.  $\varepsilon_w = 0.2$  and b.  $\varepsilon_w = 0.4$ . Predictions:  $\blacktriangle$ ,  $B = 15$  cm;  $\bullet$ ,  $B = 20$  cm;  $\blacklozenge$ ,  $B = 30$  cm. Experiments:  $\triangle$ ,  $B = 15$  cm;  $\circ$ ,  $B = 20$  cm;  $\diamond$ ,  $B = 30$  cm.

The good agreements between the numerical results and the experimental data of different researchers show that the present mathematical model is reliable for predicting the reflection coefficients of regular and irregular waves from perforated caisson breakwaters.

## 4 Discussion

### 4.1 Effect of rock fill

For the limiting case of  $f_r = +\infty$  and  $\varepsilon_w = 0$ , the reflection coefficient  $K_r$  of regular waves is mainly affected by the factors of  $B/L$ ,  $G$ ,  $h/L$  and  $b/h$ ,

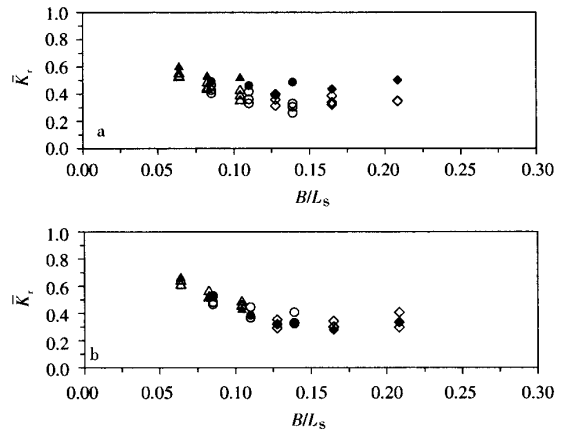


Fig. 8. Comparison of irregular wave reflection coefficients between present predictions and experimental results. a.  $\varepsilon_w = 0.2$  and b.  $\varepsilon_w = 0.4$ . Predictions:  $\blacktriangle$ ,  $B = 15$  cm;  $\bullet$ ,  $B = 20$  cm;  $\blacklozenge$ ,  $B = 30$  cm. Experiments:  $\triangle$ ,  $B = 15$  cm;  $\circ$ ,  $B = 20$  cm;  $\diamond$ ,  $B = 30$  cm.

which has been carefully investigated in the past (Sahoo, 2000; Li et al. 2002). For the present structure, our primary numerical results indicate that the effects of these factors on the reflection coefficient of regular wave are similar to the limiting case. Therefore we only examine the effect of rock fill property, which is identified by  $f_r$  and  $\varepsilon_r$ , on the reflection coefficient of regular and irregular waves in this study.

Figure 9 shows the effect of rock fill on the reflection coefficient of regular waves for  $k_0 h = 1.3$ ,  $b/h = 0.5$ ,  $\delta/h = 0.025$ ,  $\varepsilon_w = 0.3$ ,  $f_w = 8.7$  and  $s_w = s_r = 1.0$ . Here the resistance coefficient  $f_r$  is simply treated as a constant. The reflection coefficient is plotted as a function of the dimensionless wave chamber width  $B/L$ . It can be seen from this figure that all waves are reflected ( $K_r = 1.0$ ) when  $B/L$  approaches 0. When  $B/L$  increases from 0.00 to 0.19, the variations of  $f_r$  and  $\varepsilon_r$  almost have no effects on the reflection coefficient of regular wave, and the reflection coefficient of regular wave reaches its minimum at about  $B/L = 0.16$ . Once  $B/L$  ex-

ceeds 0.19, the effects of  $f_r$  and  $\varepsilon_r$  on the reflection coefficient of regular wave will tend to be significant. It is also noted that as  $f_r$  increases and  $\varepsilon_r$  decreases, the maximum value of the reflection coefficient increases. The total reflection can be observed at  $B/L$  about equaling 0.39 for the limiting case of  $f_r = +\infty$  and  $\varepsilon_r = 0$ . In practice, the resistance coefficient and the porosity of rock fill cannot be varied substantially. The typical values of  $f_r$  and  $\varepsilon_r$  are about 2.0 (Yu, 1995) and 0.4 ~ 0.5 (Isaacson et al., 2000). In addition, the value of  $B/L < 0.25$  is more common in practice. Therefore, detailed consideration on the choice of rock fill may be not necessary for practical engineering constructions.

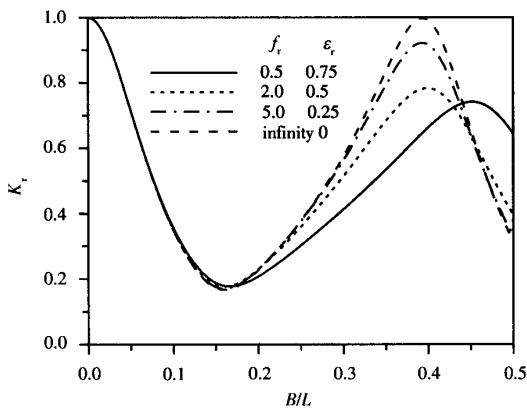


Fig. 9. Effect of rock fill on the reflection coefficient of regular waves.

Figure 10 shows the effect of rock fill on the reflection coefficient of irregular waves. The incident wave spectrum used here is the modified JONSWAP spectrum (Goda, 1999) with  $\gamma = 3.3$ . In the calculations, the value of  $\bar{k}_0 h = 1.3$  is used, where  $\bar{k}_0$  is the wavenumber corresponding to the mean irregular wavelength ( $\bar{L}$ ). The other conditions are the same as Fig. 9. By comparing Figs 10 and 9, the effects of rock fill on  $\bar{K}_r$  and  $K_r$  are much similar. It should be mentioned that except for  $B/L_s = 0$ , the total reflection of irregular waves does not occur even for the limiting case of  $f_r = +\infty$  and  $\varepsilon_r = 0$ .

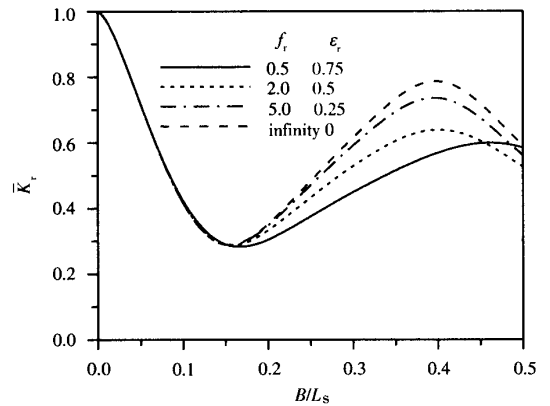


Fig. 10. Effect of rock fill on the reflection coefficient of irregular waves.

#### 4.2 Differences between regular and irregular waves

Since the reflection coefficients of regular and irregular waves can both be predicted by means of the present mathematical model, it is natural to give a comparison between them. This should be interesting and useful. In the comparison, the wave period of regular waves is determined to equal the mean period of irregular waves, which seems to be a reasonable choice. Figure 11 shows the comparison between regular and irregular waves for the cases of  $k_0 h = \bar{k}_0 h = 1.3$ ,  $b/h = 0.5$ ,  $\delta/h = 0.025$ ,  $f_w = 8.7$ ,  $f_r = 2.0$ ,  $s_w = s_r = 1.0$  and  $\varepsilon_w = 0.2$  and  $0.4$ , respectively. Here two different incident wave spectra are used for irregular waves. One is the modified JONSWAP spectrum (Goda, 1999), and the other is the B - M spectrum as follows (Yu, 2000):

$$S_i(f') = 0.257 H_s^2 T_s^{-4} f'^{-5} \exp[-1.03 (T_g f')^{-4}]. \tag{27}$$

From Fig. 11, it can be seen again that all waves are reflected when  $B/L$  (or  $B/\bar{L}$ ) approaches 0. As the increasing value of  $B/L$  (or  $B/\bar{L}$ ), the reflection coefficient oscillates between its minimum and maximum for both regular and irregular waves. It can also be seen that the minimum  $\bar{K}_r$  is larger than the minimum  $K_r$ , but the maximum  $\bar{K}_r$  is smaller than the maximum  $K_r$ . The reflection coefficient

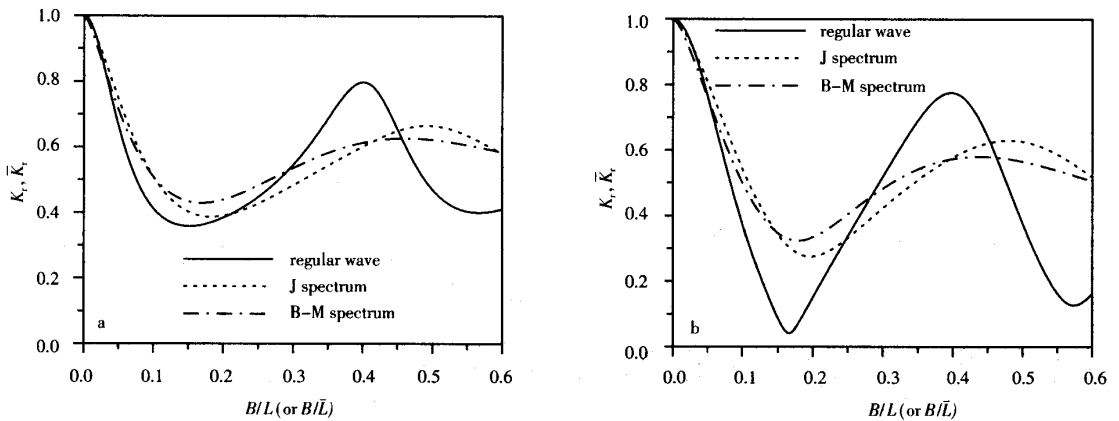


Fig. 11. Comparison of predicted reflection coefficients between regular and irregular waves. a.  $\epsilon_w = 0.2$  and b.  $\epsilon_w = 0.4$ .

of irregular waves is actually the frequency average value as defined in Eq. (22). Therefore, the value of  $\bar{K}_r$  cannot reach too large or small compared with  $K_r$ . By further investigating the curves of irregular waves in Fig. 11, the minimum  $\bar{K}_r$  of the B - M spectrum is larger than that of the JONSWAP spectrum, but the contrary is the case for the maximum  $\bar{K}_r$ . This is due to the fact that the wave energy distribution of different component waves of the B - M spectrum is more moderate than that of the JONSWAP spectrum. It can also be seen from Fig. 11 that, as for the practical condition of  $B/L < 0.25$ , the reflection coefficient of irregular waves is generally larger than regular waves. Therefore, the irregular wave model is recommended for practice.

The present experimental data given in Figs 7 and 8 are also used to examine the differences be-

tween regular and irregular waves. In our experiments, there are a total of seven different wave factors corresponding to regular and irregular waves, which can be used for the comparison. These wave factors are all listed in Table 2. They are chosen according to  $T \approx \bar{T}$  and  $H \approx H_{1\%}$ , where  $\bar{T} = T_s/1.15$  and the relation between  $H_{1\%}$  and  $H_s$  can be found in Yu (2000). The comparison between regular and irregular waves based on our experimental data is shown in Fig. 12. Generally, the measured reflection coefficients of irregular waves are larger than the corresponding results of regular waves under experimental conditions. This is consistent with the above numerical results. Moreover, the differences between  $\bar{K}_r$  and  $K_r$  for  $\epsilon_w = 0.4$  are usually larger than that of  $\epsilon_w = 0.2$ , especially in the range of  $B/L = 0.13 \sim 0.17$ . This can also be easily observed in Fig. 11.

Table 2. Wave factors used for the comparison between regular and irregular waves

Regular waves								Irregular waves							
$T/s$	1.2	1.0	0.86	1.2	1.0	1.2	1.0	$T_r/s$	1.38	1.15	0.99	1.38	1.15	1.38	1.15
$H/cm$	8	8	8	10	10	12	12	$H_r/cm$	5.3	5.3	5.3	6.7	6.7	8.0	8.0

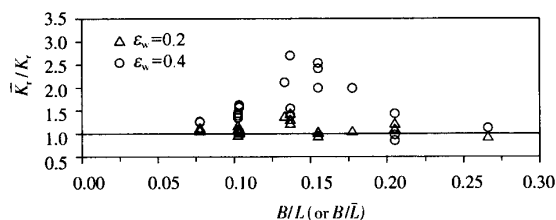


Fig. 12. Comparison of measured reflection coefficients between regular and irregular waves.

## 5 Conclusions

An analytical model is developed in this paper to examine the reflection coefficients of regular and irregular waves from a partially perforated caisson breakwater with a rock-filled core. The numerical results of the present model for two limiting cases are exactly the same as the predictions of previous analytical models. The present model is also validated by comparing the present predictions with the experimental data of different researchers. The effect of rock fill on the reflection coefficient is examined and it is not important for the current engineering practice ( $B/L < 0.25$ ). Moreover, the differences between regular and irregular waves are investigated. The minimum reflection coefficient of irregular waves is larger than that of the corresponding regular waves, but the contrary is the case for the maximum reflection coefficient. This is due to the fact that the reflection coefficient of irregular waves is the frequency average result. For the practical condition of  $B/L < 0.25$ , the reflection coefficients of irregular waves are generally larger than the corresponding results of regular waves. Thus the irregular wave model is recommended for practice.

## Acknowledgements

This study was financially supported by the Program for Changjiang Scholars and Innovative Re-

search Teams in Universities of China under contract No. IRT0420.

## References

- Bennett G S, McIver P, Smallman J V. 1992. A mathematical model of a slotted wavescreen breakwater. *Coastal Engineering*, 18: 231 ~ 249
- Chen Xuefeng, Li Yucheng, Sun Dapeng, et al. 2002. The experimental study of reflection coefficient and wave forces acting on perforated caisson. *Acta Oceanologica Sinica*, 21(3): 451 ~ 460
- Chwang A T. 1983. A porous - wavemaker theory. *J Fluid Mech*, 132: 395 ~ 406
- Chwang A T, Dong Z. 1984. Wave - trapping due to a porous plate. In: 15th Symp on Naval Hydrodynamics. Hamburg: Session VI. 32 ~ 42
- Fugazza M, Natale L. 1992. Hydraulic design of perforated breakwaters. *Journal of Waterway, Port, Coastal, and Ocean Engineering*, ASCE, 118(1): 1 ~ 14
- Goda Y. 1999. A comparative review on the functional forms of directional wave spectrum. *Coastal Engineering Journal*, 41(1): 1 ~ 20
- Isaacson M, Baldwin J, Allyn N, et al. 2000. Wave interactions with perforated breakwater. *Journal of Waterway, Port, Coastal, and Ocean Engineering*, ASCE, 126(5): 229 ~ 235
- Jarlan G E. 1961. A perforated vertical wall breakwater. *The Dock and Harbour Authority*, XII (486): 394 ~ 398
- Li Yucheng, Liu Hongjie, Dong Guohai. 2005. The force of oblique incident wave on the breakwater with a partially perforated wall. *Acta Oceanologica Sinica*, 24(4): 121 ~ 130
- Li Yucheng, Liu Yong, Teng Bin. 2006. Porous effect parameter of thin permeable plates. *Coastal Engineering Journal*, 48(4): 309 ~ 336
- Li Yucheng, Liu Hongjie, Teng Bin, et al. 2002. Reflection of oblique incident waves by breakwaters with partially-perforated wall. *China Ocean Engineering*, 16(3): 329 ~ 342
- Liu Yong, Li Yucheng, Teng Bin, et al. 2006. Experimental and theoretical investigation of wave forces on a partially-perforated caisson breakwater with a rock-filled core. *China Ocean Engineering*, 20(2): 179 ~ 198
- Requejo S, Vidal C, Losada I J. 2002. Modelling of wave loads and hydraulic performance of vertical permeable structures. *Coastal Engineering*, 46: 249 ~ 276
- Sahoo T, Lee M M, Chwang A T. 2000. Trapping and genera-

- tion of waves by vertical porous structures. *Journal of Engineering Mechanics*, ASCE, 126(10):1 074 ~ 1 082
- Sollit C K, Cross R H. 1972. Wave transmission through porous breakwaters. In: Proc of the 13th Coastal Eng Conf. Vancouver: ASCE, 1 827 ~ 1 846
- Song Jinbao, Sun Qun. 2006. Second-order random interfacial wave solutions for two-layer fluid with a free surface. *Acta Oceanologica Sinica*, 25(1):15 ~ 20
- Suh K D, Choi J C, Kim B H, et al. 2001. Reflection of irregular waves from perforated-wall caisson breakwaters. *Coastal Engineering*, 44:141 ~ 151
- Suh K D, Park J K, Park W S. 2006. Wave reflection from partially perforated-wall caisson breakwater. *Ocean Engineering*, 33: 264 ~ 280
- Tanimoto K, Haranaka S, Takahashi S, et al. 1976. An experimental investigation of wave reflection, overtopping and wave forces for several types of breakwaters and sea walls. In: Technical Note of Port and Harbour Research Institute (in Japanese). n246. Japan: Ministry of Transport
- Tanimoto K, Yoshimoto Y. 1982. Theoretical and experimental study of reflection coefficient for wave dissipating caisson with a permeable front wall. Report of the Port and Harbour Research Institute (in Japanese), 21(3): 44 ~ 77
- Teng Bin, Gou Ying, Cheng Liang, et al. 2006. Draft effect on wave action with a semi-infinite elastic plate. *Acta Oceanologica Sinica*, 25(6): 116 ~ 127
- Twu S W, Lin D T. 1991. On a highly effective wave absorber. *Coastal Engineering*, 15: 389 ~ 405
- Van Gent M R A. 1995. Wave interaction with permeable coastal structures: [dissertation]. Delft: Delft University of Technology, 22 ~ 46
- Yu Xiping. 1995. Diffraction of water waves by porous breakwaters. *Journal of Waterway, Port, Coastal, and Ocean Engineering*, ASCE, 121(6): 275 ~ 282
- Yu Yuxiu. 2000. Random Wave and Its Applications for Engineering (in Chinese). Dalian: Dalian University of Technology Press